

Righi-Leduc effect in Y- and Bi-based high-T_c superconductors

B. Zeini, A. Freimuth, B. Büchner, R. Gross, Arno P. Kampf, M. Kläser, G. Müller-Vogt

Angaben zur Veröffentlichung / Publication details:

Zeini, B., A. Freimuth, B. Büchner, R. Gross, Arno P. Kampf, M. Kläser, and G. Müller-Vogt. 2000. "Righi-Leduc effect in Y- and Bi-based high-T_c superconductors." *Physica C: Superconductivity* 317-318: 325-32. [https://doi.org/10.1016/S0921-4534\(99\)00076-3](https://doi.org/10.1016/S0921-4534(99)00076-3).

Righi–Leduc effect in Y- and Bi-based high- T_c superconductors

B. Zeini ^a, A. Freimuth ^{a,*}, B. Büchner ^a, R. Gross ^a, A.P. Kampf ^b, M. Kläser ^c,
G. Müller-Vogt ^c

^a *II. Physikalisches Institut, Universität zu Köln, 50937 Cologne, Germany*

^b *Theoretische Physik III, Elektronische Korrelationen und Magnetismus, Institut für Physik, Universität Augsburg, 86135 Augsburg, Germany*

^c *Kristall- und Materiallabor, Universität Karlsruhe, 76128 Karlsruhe, Germany*

Abstract

Measurements of the transverse (k_{xy}) and longitudinal (k_{xx}) thermal conductivity in the superconducting state of single crystals of $\text{YBa}_2\text{Cu}_3\text{O}_{7-\delta}$ (YBCO) and $\text{Bi}_2\text{Sr}_2\text{CaCu}_2\text{O}_{8-\delta}$ (BSCCO) are presented in applied magnetic fields up to 14 T. We separate the electronic thermal conductivity (k_{xx}^{el}) of the CuO_2 -planes from the phononic thermal conductivity (k_{xx}^{ph}) using k_{xy} and the magnetic field dependence of k_{xx} . Our main results are: (1) In YBCO $k_{xx}^{\text{el}}(T)$ shows a pronounced maximum. We attribute this to a rapid increase of the quasiparticle scattering time τ below T_c . The maximum of $k_{xx}^{\text{el}}(T)$ in BSCCO is much smaller due to stronger impurity scattering. The maximum of k_{xx} is strongly suppressed by a magnetic field, presumably because of scattering of QPs on vortices. (2) Our data analysis reveals that below T_c a transport (τ) and Hall (τ_H) relaxation time must be distinguished as in the normal state. Whereas τ is strongly enhanced below T_c , τ_H displays the same temperature dependence as above T_c .

Keywords: Righi–Leduc effect; Thermal conductivity; Single crystal

1. Introduction

A characteristic feature of the high- T_c superconductors (HTSC) is a pronounced maximum of their thermal conductivity k_{xx} in the superconducting state [1–4]. On the one hand, this maximum has been attributed to the quasiparticle (QP) contribution to the thermal conductivity, resulting from a strong suppression of the QP scattering rate below T_c ,

which overcompensates the decrease of the number of QPs [3,5,6]. Alternatively, the maximum has been attributed to the phononic contribution k_{xx}^{ph} to the thermal conductivity [1,2]. It is well known from conventional superconductors that the scattering of phonons on electrons is reduced in the superconducting state, when electrons condense into the superfluid [1]. In order to settle this issue, a separation of the QP and phonon heat currents is required. This is up to now an open problem.

It has been pointed out in Refs. [7–9] that the transverse thermal conductivity k_{xy} , also called the Righi–Leduc or thermal Hall effect, has no phonon contribution, i.e., k_{xy} is purely electronic. One there-

* Corresponding author. Fax: +49-221-470-3596; E-mail: freimuth@ph2.uni-koeln.de

fore expects to gain direct information on the QP relaxation time from the measurement of k_{xy} . However, in the cuprates additional complications arise when effects transverse in a magnetic field such as the Hall and Righi–Leduc effect are involved. The study of the normal state electrical transport phenomena clearly showed that a consistent interpretation of the experimental data requires a distinction of two relaxation times [10–12]: whereas a longitudinal (transport) relaxation time τ enters the dc conductivity, $\sigma_{xx} \propto \tau$, a transverse Hall relaxation time τ_H is necessary to describe the Hall conductivity $\sigma_{xy} \propto \tau\tau_H$ and thus the Hall angle $\tan \alpha_H = \sigma_{xy}/\sigma_{xx} \propto \tau_H^{-1}$.

In this paper, we present a detailed study of k_{xx} and k_{xy} of single crystals of $\text{YBa}_2\text{Cu}_3\text{O}_{7-\delta}$ and $\text{Bi}_2\text{Sr}_2\text{CaCu}_2\text{O}_{8+\delta}$. Our data analysis shows that a distinction of two relaxation times is also necessary for the description of thermal transport properties both, in the normal and in the superconducting state. In particular, τ is strongly enhanced below T_c and becomes magnetic field dependent, whereas τ_H shows the same magnetic field and temperature dependence as in the normal state. We also separate the QP and phononic contribution to the heat current using k_{xy} and the magnetic field dependence of k_{xx} .

2. The Righi–Leduc effect

The thermal conductivity tensor \underline{k} is defined via the heat current density:

$$\mathbf{j}_h = -\underline{k}\nabla T. \quad (1)$$

Here, \underline{k} is the sum of an electronic and a phononic part:

$$\underline{k} = \underline{k}^{\text{el}} + \underline{k}^{\text{ph}}. \quad (2)$$

It is natural to assume that $\underline{k}^{\text{ph}}$ remains diagonal even for $\mathbf{B} \neq 0$, i.e., $k_{xy}^{\text{ph}} = 0$. In this case the transverse components of \underline{k} are purely electronic. The transverse thermal conductivity is the thermal analogue of the Hall effect and is measured as follows: in a magnetic field $\mathbf{B} = (0, 0, B)$ a temperature gradient $\nabla_x T$ is applied in the x -direction. Under the condition $j_{h,y} = 0$ a transverse temperature gradient

$\nabla_y T$ is found in the y -direction. Using the Onsager relations we find in this situation

$$j_{h,y} = k_{xy}\nabla_x T - k_{xx}\nabla_y T = 0 \quad (3)$$

with $k_{xx} = k_{yy}$ for twinned crystals without in-plane anisotropy. Hence, k_{xy} can be determined experimentally by measuring $\nabla_x T$, $\nabla_y T$, and the *total* longitudinal thermal conductivity k_{xx} .

According to standard transport theory $\underline{k}^{\text{el}}$ is related to the conductivity tensor $\underline{\sigma}$ via the Wiedemann–Franz law (see, for example, Ref. [13])

$$\underline{k}^{\text{el}} = L T \underline{\sigma}, \quad (4)$$

where L is the Lorenz number. This relation implies that the thermal and electrical Hall angles, $\tan \alpha_R = k_{xy}/k_{xx}^{\text{el}}$ and $\tan \alpha_H = \sigma_{xy}/\sigma_{xx}$ are equal.

3. Experimental

Our measurements were carried out at constant temperatures with the magnetic field applied perpendicular to the CuO_2 -planes and all temperature gradients within the CuO_2 -planes. Typically, temperature gradients $\nabla_x T$ of the order of 0.5 K/mm were applied using a small manganin heater mounted on top of the samples (Fig. 1). The resulting transverse temperature gradients $\nabla_y T$ of about 10^{-3} K/mm were measured with AuFe–Chromel thermocouples in magnetic fields up to 14 T. The thermocouples were calibrated in the same field range (1) with an α -quartz crystal and (2) against a thermocouple placed in zero field, but kept at the same temperature difference (for details see Ref. [14,15]). To eliminate offset voltages due to misalignment of the thermocouple $\nabla_y T$ was measured for both field directions $\pm \mathbf{B}$, since the Righi–Leduc component of $\nabla_y T$ must be antisymmetric with respect to field reversal. We have measured in two different modes: Either \mathbf{B} was reversed at fixed temperature or the sample was heated up to temperatures above T_c before the field was reversed. In order to avoid hysteresis as observed in Ref. [16], e.g., due to vortex pinning effects this latter mode was used for all low temperature measurements. We have tested our method by measurements on an insulator ($k_{xy} = 0$) and on sim-

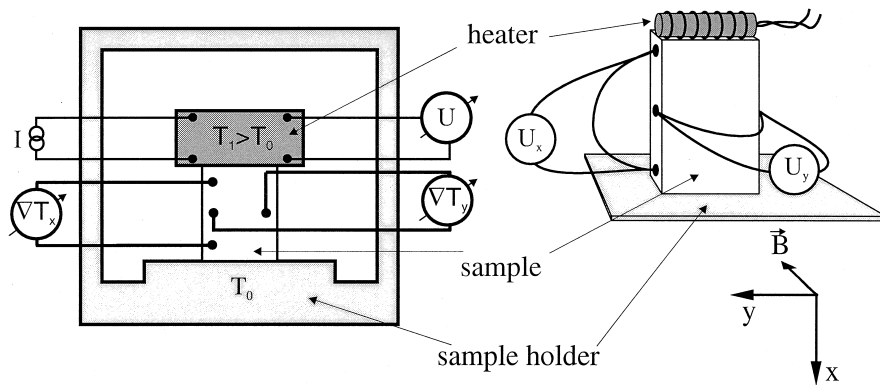


Fig. 1. Schematic setup used for the measurements (see text).

ple metals. Details of our experimental setup will be described elsewhere [14,15].

The results presented here have been obtained on a high quality twinned single crystal of $\text{YBa}_2\text{Cu}_3\text{O}_{7-\delta}$ (YBCO) ($a \approx b \approx 2$ mm; $c \approx 0.4$ mm) with a superconducting transition at $T_c \approx 90.5$ K and on a single crystal of $\text{Bi}_2\text{Sr}_2\text{CaCu}_2\text{O}_{8+\delta}$ (BSCCO) ($a \approx b \approx 1$ mm; $c \approx 0.05$ mm) with $T_c \approx 80$ K.

4. Results

The thermal conductivity k_{xx} of the YBCO sample in zero magnetic field as a function of temperature is shown in Fig. 2. The absolute value of k_{xx} at T_c is of the order of 10 W/K m. k_{xx} increases drastically below T_c and reaches a maximum at ≈ 40 K. The normal state thermal conductivity is independent of the magnetic field within our experimental resolution. In contrast, k_{xx} is strongly suppressed by a magnetic field below T_c . The magnetic field dependence of k_{xx} is shown in Fig. 4, where we plot $\Delta k_{xx} = k_{xx}(B) - k_{xx}(B=0)$ as a function of the magnetic field at fixed temperatures. k_{xx} varies non-linearly with B . Moreover, the magnetic field dependence changes with temperature: at the lowest temperatures measured, k_{xx} has a tendency to become magnetic field independent at high fields. This is reminiscent of the behavior reported recently by Krishana et al. [17] for BSCCO.

In Fig. 3, k_{xy} is plotted vs. temperature. k_{xy} is positive and of the order 10^{-2} (W/K m) for $B \approx 1$

T. It exhibits a pronounced maximum below T_c . The position of this maximum shifts slightly to higher temperatures with increasing magnetic field from about 40 K at $B = 3$ T to nearly 50 K at $B = 14$ T. Comparing k_{xy} to k_{xx} one notes that the maximum

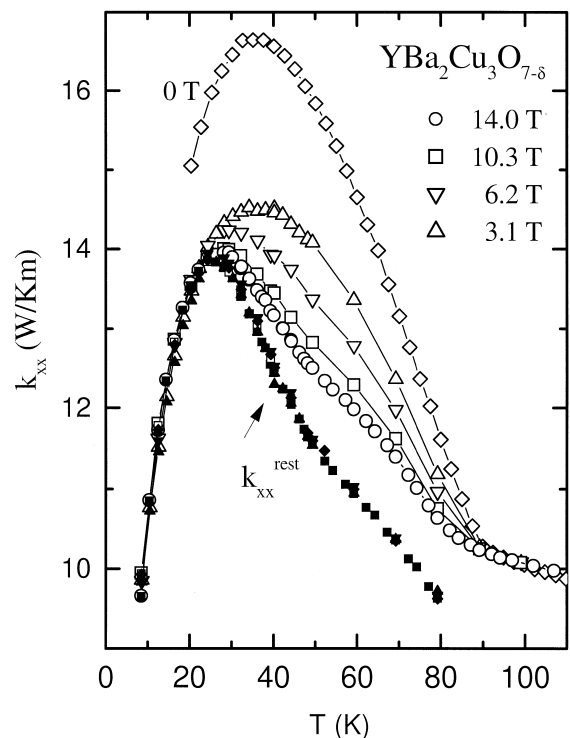


Fig. 2. Longitudinal thermal conductivity of YBCO vs. temperature at fixed magnetic fields given in the figure. Solid symbols: k_{xx}^{rest} as obtained from our data analysis (see text).

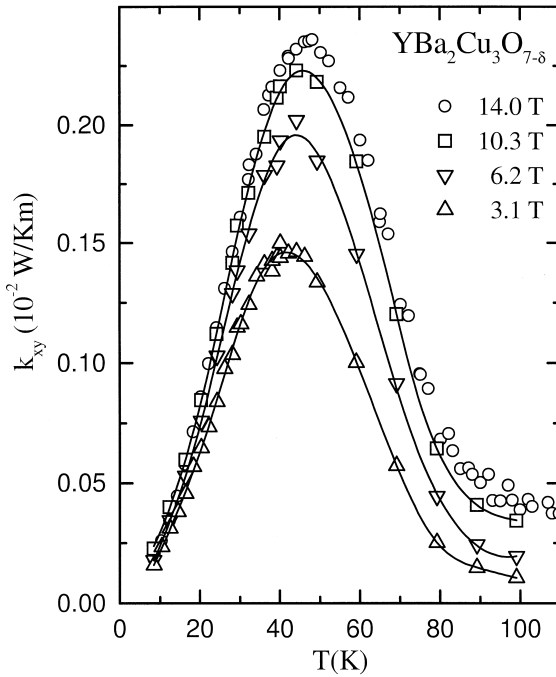


Fig. 3. Transverse thermal conductivity of YBCO vs. temperature at fixed magnetic fields given in the figure.

in $k_{xy}(T)$ occurs at a higher temperature and that the relative increase in $k_{xy}(T)$ below T_c is much larger. Comparing the absolute value of $k_{xy}(T_c)$ to $k_{xx}(T_c)$

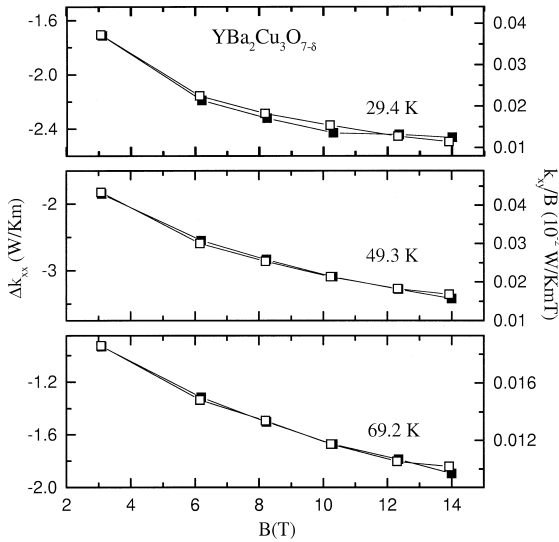


Fig. 4. $\Delta k_{xx} \equiv k_{xx}(B) - k_{xx}(B=0)$ (■) and k_{xy}/B (□) vs. magnetic field at fixed temperatures given in the figure.

≈ 10 W/K m reveals that the thermal Hall angle at 1 T is less than 10^{-3} . A quantitative determination is not possible at this point, since k_{xx} is dominated by the phonon contribution.

The magnetic field dependence of k_{xy} is also shown in Fig. 4, where we show k_{xy}/B . We emphasize that the magnetic field dependencies of k_{xx} and of k_{xy}/B are identical within our experimental accuracy, which implies that

$$\frac{\partial}{\partial B} \left(\frac{k_{xy}}{B} \right) \propto \frac{\partial k_{xx}}{\partial B}. \quad (5)$$

At the lowest temperatures used in our experiments k_{xy} has the tendency to become independent of B at high magnetic fields above 3 T. We note that the data of Fig. 4 are similar to the results of a previous study [8]. On the other hand, we do not find a decrease of k_{xy} with increasing B at high magnetic fields, in contrast to what is reported in Ref. [18].

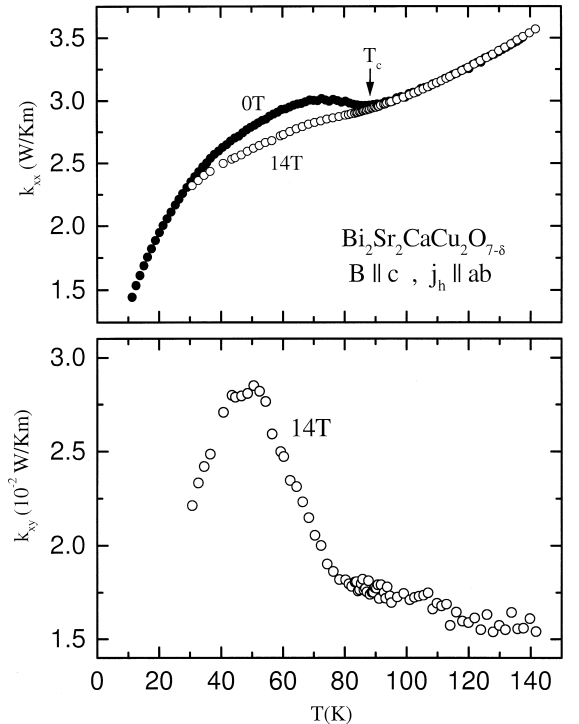


Fig. 5. Longitudinal (upper panel) and transverse (lower panel) thermal conductivity of BSCCO vs. temperature for fixed magnetic fields given in the figure.

The thermal conductivity of BSCCO is shown in the upper panel of Fig. 5. k_{xx} is of order 3 W/K m near T_c . This value is significantly smaller than that found for YBCO. Below T_c in zero magnetic field a weak upturn in $k_{xx}(T)$ is observed with a maximum around 70 K. This maximum is almost completely suppressed when applying a magnetic field of 14 T.

k_{xy} measured on this sample is shown in the lower panel of Fig. 5. The behavior of k_{xy} is qualitative similar to that found in YBCO. In particular, although the maximum of $k_{xx}(T)$ below T_c is hardly visible for BSCCO, $k_{xy}(T)$ clearly shows a pronounced maximum at about 50 K. However, note that in BSCCO the absolute magnitude of $k_{xy}(14\text{ T})$ is smaller by about a factor of 4 in the normal state just above T_c and that the maximum value of $k_{xy}(T)$ below T_c is smaller by a factor of about 10.

5. Data analysis and discussion

For our analysis, we assume that k_{xx} is the sum of three contributions¹

$$k_{xx} = k_{xx}^{\text{el}} + k_{xx}^{\text{ch}} + k_{xx}^{\text{ph}} = k_{xx}^{\text{el}} + k_{xx}^{\text{rest}}. \quad (6)$$

Here, k_{xx}^{el} is the electronic thermal conductivity of the CuO_2 -planes (in fact, bilayers in YBCO and BSCCO) and k_{xx}^{ph} is the phononic thermal conductivity. k_{xx}^{ch} must be included in the data analysis only if an additional electronic channel of heat conduction is present with a magnetic field or temperature dependence *different* from that of k_{xx}^{el} . Such a situation is most probably realized in YBCO, where in addition to the CuO_2 -planes (pl) common to all HTSCs, CuO-chains (ch) are present along the b -direction of the orthorhombic crystal structure. In untwinned crystals, these chains lead to significant a - b anisotropy of the electronic properties. Note that a contribution from the chains to the longitudinal transport properties is present even for twinned samples, where an in-plane average of k_{xx}^{ch} contributes. Since the CuO-chains form a one-dimensional channel of conduction the magnetic field and temperature depen-

dence of k_{xx}^{ch} may be different from that of k_{xx}^{el} . In particular, one expects no magnetic field dependence. Moreover, the CuO-chains should not contribute to the transverse effects.

5.1. Thermal Hall angle

We relate the transverse and longitudinal electronic thermal conductivity (of the CuO_2 -planes) according to

$$k_{xy} = k_{xx}^{\text{el}} \tan \alpha_R = k_{xx}^{\text{el}} \omega_c \tau_R. \quad (7)$$

This equation defines a ‘relaxation time’ $\tau_R(T, B)$, which is used to parametrize the temperature and magnetic field dependence of the thermal Hall angle. The distinction between τ and τ_R is of course motivated by the distinction between τ and τ_H required for the description of the electrical transport properties in the normal state. Nevertheless, at this point we leave open, whether τ_R must be identified with the transport or the Hall relaxation time in order to demonstrate that the subsequent analysis is independent of this.

The key experimental observation underlying our analysis is that $\Delta k_{xx} = k_{xx}(B) - k_{xx}(B=0)$ and k_{xy}/B have the same magnetic field dependence, as expressed by Eq. (5). To understand the implication of this result, we note that Eqs. (7) and (6) yield

$$\begin{aligned} \frac{m}{e} \frac{\partial}{\partial B} \left(\frac{k_{xy}}{B} \right) &= \tau_R \frac{\partial k_{xx}^{\text{el}}}{\partial B} + k_{xx}^{\text{el}} \frac{\partial \tau_R}{\partial B} \\ &= \tau_R \frac{\partial k_{xx}}{\partial B} + \left[k_{xx}^{\text{el}} \frac{\partial \tau_R}{\partial B} - \tau_R \frac{\partial k_{xx}^{\text{ph}}}{\partial B} - \tau_R \frac{\partial k_{xx}^{\text{ch}}}{\partial B} \right]. \end{aligned} \quad (8)$$

Apparently, our experimental results, i.e., Eq. (5), imply that the term in brackets is zero. Since the three terms in brackets refer to three different channels of heat conduction, this requires that τ_R , k_{xx}^{ph} , and k_{xx}^{ch} are separately field independent.

With these results and using Eqs. (8) and (7) τ_R can be determined according to

$$\frac{e}{m} \tau_R = \frac{\partial}{\partial B} \left(\frac{k_{xy}}{B} \right) \bigg/ \frac{\partial k_{xx}}{\partial B} = \frac{\Delta(k_{xy}/B)}{\Delta k_{xx}}. \quad (9)$$

The result of this analysis is shown in Fig. 6 for YBCO.

¹ We note that vortex motion contributes to the heat current below T_c . This contribution is, however, small compared to the heat carried by the QPs (see, e.g., Refs. [14,15]).

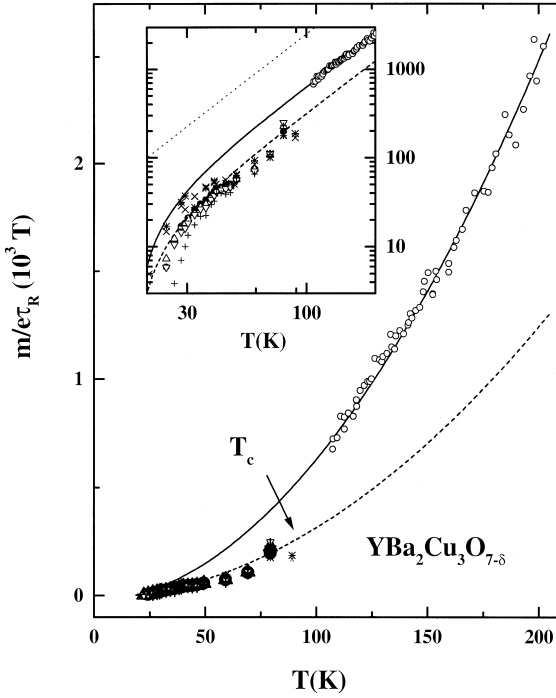


Fig. 6. $m/e\tau_R$ vs. temperature T . $T < T_c$: Data are obtained from Eq. (9) with $\Delta(k_{xy}/B) \equiv k_{xy}(B_1)/B_1 - k_{xy}(B_2)/B_2$ and $\Delta k_{xx} \equiv k_{xx}(B_1) - k_{xx}(B_2)$. Different symbols correspond to different values of B_1 and B_2 . $T > T_c$: $m/e\tau_H$ obtained from σ_{xy} and σ_{xx} . Solid line: extrapolated normal state data. Dashed line: extrapolated normal state data divided by a factor 2 (see text). Inset: The same data on a double logarithmic scale. The solid and dashed lines have the same meaning as the above. The dotted line corresponds to $\tau_R^{-1} \propto T^2$.

As a check of our result for τ_R , we have also determined $e\tau_H/m = \sigma_{xy}/B\sigma_{xx}$ for the same sample from measurements of σ_{xy} and σ_{xx} in the normal state [14,15]. These data as well as their extrapolation² to temperatures below T_c are also shown in Fig. 6. Comparing the extrapolated values for τ_H^{-1} to τ_R^{-1} we find that the temperature dependence is similar, approximately a T^2 -dependence. However, τ_R appears to be systematically smaller by about a factor of 2. Although we do not regard this factor of 2 as important, we note that it can be

² We have fitted the resistivity ρ and the inverse Hall coefficient R_H^{-1} to $a + bT$ and to $\tilde{a} + \tilde{b}T$, respectively, where a , b , \tilde{a} , and \tilde{b} are constants. $e\tau_H/m$ was then obtained from $e\tau_H/m = \sigma_{xy}/B\sigma_{xx} \approx R_H/\rho = [(a + bT)(\tilde{a} + \tilde{b}T)]^{-1}$.

explained in a straightforward way: we first note that τ_R as extracted from the thermal transport data is clearly unaffected by the CuO-chains and that this is also true for σ_{xy} . In contrast, σ_{xx} has a contribution from the CuO-chains, i.e., $\sigma_{xx} = \sigma_{xx}^{\text{pl}} + \langle \sigma_{xx}^{\text{ch}} \rangle$, where σ_{xx}^{pl} is the electrical conductivity of the CuO₂-planes and $\langle \sigma_{xx}^{\text{ch}} \rangle$ is an average of the chain contribution appropriate for a twinned crystal. With $\sigma_{xx}^{\text{pl}} \approx \langle \sigma_{xx}^{\text{ch}} \rangle$ [12], we conclude that $e\tau_H/m = \sigma_{xy}/B\sigma_{xx}$ is underestimated by a factor of 2. Correcting the normal state data for this factor, we find excellent agreement between τ_H and τ_R , i.e., our data suggest $\tau_R \approx \tau_H$.

We thus arrive at an important result of our analysis: our data show clearly that $\tau_R \approx \tau_H$ and that —anticipating our results for $\tau - \tau_H$ and τ behave differently also below T_c in the same way as in the normal state. In particular, τ_H is unaffected by the superconducting transition and shows the same temperature dependence as above T_c , whereas τ is strongly suppressed below T_c . This finding should provide important information for the theoretical understanding of transport phenomena in the cuprates.

5.2. Electronic thermal conductivity

Once τ_R is known, the remainder of our analysis is straightforward: $k_{xx}^{\text{el}} (B \neq 0)$ follows from Eq. (7) using the data for $k_{xy}(B)$. Subsequently, k_{xx}^{rest} is obtained from Eq. (6) for each field strength. As a test of consistency, we have verified that k_{xx}^{rest} is indeed field independent. Finally, knowing k_{xx}^{rest} the zero field electronic thermal conductivity $k_{xx}^{\text{el}} (B = 0)$ follows from Eq. (6) using the zero field data for k_{xy} . We have also determined $k_{xx}^{\text{el}} (B = 0)$ directly from Eq. (7) using an extrapolation of B/k_{xy} to $B = 0$ in good agreement with the results obtained from using k_{xx}^{rest} and Eq. (6).

In the lower panel of Fig. 7, we show $k_{xx}^{\text{el}}(B)$ as obtained from our data analysis for YBCO. k_{xx}^{el} represents the electronic thermal conductivity of the CuO₂-planes in YBCO. Our results confirm explicitly that k_{xx}^{el} is strongly enhanced below T_c . Since $k_{xx}^{\text{el}} \propto T n_{\text{QP}} \tau$ this implies that τ is strongly enhanced below T_c overcompensating the decrease of the QP number density $n_{\text{QP}}(T)$ with decreasing temperature. This confirms the results obtained for the QP relaxation time from the microwave conductivity [5,6]. In the upper panel, k_{xx}^{el} for BSCCO is shown. Since the field dependence of k_{xx}^{el} is much weaker in BSCCO,

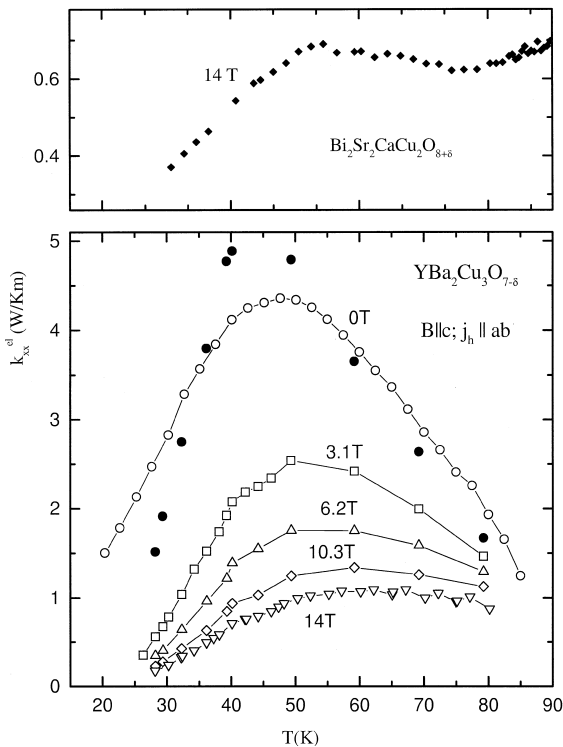


Fig. 7. Electronic thermal conductivity k_{xx}^{el} of the CuO_2 -planes as a function of temperature for fixed magnetic fields given in the figure. Upper panel: BSCCO; lower panel: YBCO. The zero field data have been obtained from $k_{xx}^{el}(B=0) = k_{xx}(B=0) - k_{xx}^{rest}$ (○) as well as from an extrapolation of B/k_{xy} to $B=0$ (●).

we have in this case assumed that τ_R is field independent below T_c in order to calculate k_{xx}^{el} from k_{xy} . The much weaker increase of k_{xx}^{el} below T_c in BSCCO should be attributed to stronger impurity scattering in this compound. However, the inelastic, temperature dependent part of the scattering rate must increase also in this compound in order to explain the increase of k_{xx}^{el} . Thus, the collapse of the inelastic scattering rate below T_c appears to be a generic property of the cuprates.

We observe that k_{xx}^{el} is very sensitive to magnetic fields below T_c . This is in contrast to what is found in the normal state, where the total thermal conductivity and thus k_{xx}^{el} is field independent. This field dependence can be attributed to scattering of QPs on vortices [19,20], with a scattering rate τ_v^{-1} proportional to the density of vortices, i.e., $\tau_v^{-1} \propto B$ [9].

k_{xx}^{rest} as obtained from our data analysis for YBCO is shown in Fig. 2. Remarkably, k_{xx}^{rest} shows a pro-

nounced maximum below T_c , too. This maximum may be due to the phononic contribution which is expected to have a maximum at low temperatures [1]. However, it may also arise from the chain contribution. The latter has previously been determined experimentally from the a - b -anisotropy of k_{xx} in detwinned single crystals of YBCO [3,21]. It was found that k_{xx}^{ch} shows a pronounced maximum below T_c with an overall temperature dependence similar to that found here for k_{xx}^{rest} [21]. Furthermore, the field independence of k_{xx}^{rest} implies that the phononic contribution k_{xx}^{ph} is independent of B . Such a conclusion has recently been drawn also on the basis of low temperature results for the thermal conductivity in Bi-based HTSC [17].

6. Summary

We have presented a separation of the QP and phononic contributions to the thermal conductivity below T_c in $\text{YBa}_2\text{Cu}_3\text{O}_{7-\delta}$ and $\text{Bi}_2\text{Sr}_2\text{CaCu}_2\text{O}_{8+\delta}$ based on measurements of the longitudinal and transverse thermal conductivity in high magnetic fields. Our data analysis shows explicitly that the QP contribution to k_{xx} is strongly enhanced below T_c and that it is the QP contribution to the heat current which is responsible for the magnetic field dependence of k_{xx} . We find that two relaxation times must be distinguished not only in the normal state but also below T_c : whereas the QP relaxation time τ is strongly enhanced below T_c and is magnetic field dependent, the Hall relaxation time τ_H remains independent of B below T_c and has the same temperature dependence as above T_c .

Acknowledgements

We are particularly grateful for stimulating discussions with W. Brenig, Ch. Bruder, P.J. Hirschfeld, T. Kopp, D. Rainer, S. Uhlenbruck, and P. Wölfle. This work was supported by the Deutsche Forschungsgemeinschaft through SFB 341.

References

- [1] C. Uher, in: D.M. Ginsberg (Ed.), Physical Properties of High Temperature Superconductors, Vol. 3. World Scientific, Singapore, 1992.

- [2] S.D. Peacor et al., Phys. Rev. B 44 (1991) 9508.
- [3] R.C. Yu, M.B. Salamon, J.P. Lu, W.C. Lee, Phys. Rev. Lett. 69 (1992) 1431.
- [4] J.L. Cohn, V.Z. Kresin, M.E. Reeves, S.A. Wolf, Phys. Rev. Lett. 71 (1993) 1657.
- [5] D.A. Bonn, W.N. Hardy, in: D.M. Ginsberg (Ed.), Physical Properties of High Temperature Superconductors, Vol. 5. World Scientific, Singapore, 1996.
- [6] D.A. Bonn et al., Phys. Rev. Lett. 47 (1992) 11314.
- [7] A. Freimuth, M. Galfy, C. Hohn, B. Zeini, J. Low Temp. Phys. 95 (1994) 383.
- [8] K. Krishana, J.M. Harris, N.P. Ong, Phys. Rev. Lett. 75 (1995) 3529.
- [9] B. Zeini, A. Freimuth, B. Büchner, R. Gross, A.P. Kampf, M. Kläser, G. Müller-Vogt, to be published (cond-mat/9809295).
- [10] T.R. Chien, Z.Z. Wang, N.P. Ong, Phys. Rev. Lett. 67 (1991) 2088.
- [11] P.W. Anderson, Phys. Rev. Lett. 67 (1991) 2092.
- [12] Y. Iye, in: D.M. Ginsburg (Ed.), Physical Properties of the High Temperature Superconductors, Vol. 3. World Scientific, Singapore.
- [13] A.A. Abrikosov, Fundamentals of the Theory of Metals, Elsevier Science Publishing, New York, 1988.
- [14] B. Zeini, Ph.D. thesis, Universität zu Köln, 1997, Shaker Verlag, Aachen, 1998, ISBN: 3-8265-3440-9.
- [15] B. Zeini et al., to be published.
- [16] H. Aubin, K. Behnia, S. Ooi, T. Tamegai, Science 280 (1998) 9a, preprint (cond-mat/9807037).
- [17] K. Krishana, N.P. Ong, Q. Li, G.D. Gu, N. Koshizuka, Science 277 (1997) 83.
- [18] S.H. Simon, P.A. Lee, Phys. Rev. Lett. 78 (1997) 1548.
- [19] M.B. Salamon et al., J. Superconductivity 8 (1995) 449.
- [20] R.M. Cleary, Phys. Rev. 175 (1968) 587.
- [21] R. Gagnon, S. Pu, B. Ellman, L. Taillefer, Phys. Rev. Lett. 78 (1997) 1976.